

Comparison of the photoredox properties of polyoxometallates and semiconducting particles



Anastasia Hiskia, Athanasios Mylonas and Elias Papaconstantinou*

Institute of Physical Chemistry, NCSR Demokritos, 153-10 Athens, Greece

Received 29th November 1999, Revised version received 8th September 2000
First published as an Advance Article on the web 28th November 2000

We demonstrate that two large categories of compounds, namely, polyoxometallates (produced by acid condensation of mainly tungstates and/or molybdates) and aggregates of various metal oxides (formed by stirring, sonication etc) have similar properties. Emphasis is given to the photocatalytic properties of the two systems. The various steps in the photocatalytic cycles are described and several examples, from both systems, have been used to demonstrate that their photocatalytic performance is similar in terms of the overall mechanism of photodecomposition of organic compounds, the intermediate species involved and the final photodegradation products (i.e., CO_2 , H_2O and inorganic anions).

1 Introduction

Unlike CrO_4^{2-} that only dimerizes upon lowering the pH of an aqueous solution, the corresponding MoO_4^{2-} and WO_4^{2-} anions form a variety of well defined metal oxygen clusters, the

so-called polyoxometallates (POM),^{1,2} the history of which goes back to early 19th century.^{1,2} Other metal oxide anions such as vanadates, niobates and tantalates also undergo condensation reactions, but, generally the species formed are not well characterized.³

Several categories of POM can be formed by careful selection of the ingredients and by adjustment of pH and temperature.² We will mention a few characteristic groups of the great variety that exist: (a) acid condensation of pure MoO_4^{2-} or WO_4^{2-} produces the so-called isopoly compounds of the general formula $\text{M}_x\text{O}_y^{q-}$. A typical example is $\text{W}_{10}\text{O}_{32}^{4-}$ [Fig. 1(C)]. (b) If the original solution contains a heteroatom, A, like phosphorus, silicon, arsenic, iron or cobalt (about 60 elements can function as heteroatoms), acid condensation produces a heteropoly compound of the general formula $\text{A}_a\text{M}_x\text{O}_y^{q-}$, for instance, $\text{PW}_{12}\text{O}_{40}^{3-}$ and $\text{P}_2\text{W}_{18}\text{O}_{62}^{6-}$ [Fig. 1(A, B)]. (c) Mixed heteropoly compounds that contain various ratios of molybdenum and tungsten arise from a solution that contains both MoO_4^{2-} and WO_4^{2-} and a heteroatom [Fig. 1(D)]. (d) By careful adjustment of pH, M–O moieties can be removed from POM and can be replaced by mainly transition metals with a variety of ligands, thus forming the transition

Anastasia Hiskia was born in Athens, Greece in 1958. She received her Diploma in Chemistry (1981) from the University of Athens and a Doctorate Degree in Chemistry (1989) from the University of Athens in collaboration with NCSR Demokritos. She worked at the General Chemical State Lab., 1983–1995, in environmental chemistry. She joined the Catalytic–Photocatalytic Processes Lab. Institute of Physical Chemistry, NCSR Demokritos in 1995. Her research interests involve Advanced Oxidation Processes, polyoxometallates and environmental analysis.

Athanasios Mylonas was born in Athens, Greece, in 1968. He received a Diploma in Chemistry from Patras University in 1990 and a Doctorate Degree in Chemistry from the National



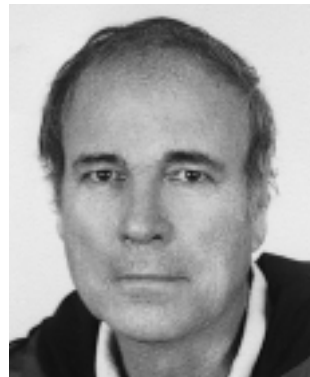
Anastasia Hiskia



Athanasios Mylonas

Technical University of Athens and NCSR Demokritos in 1996. Now he works as adjunct research scientist at NCSR Demokritos and as Director of Research and Development at Chemo Hellas.

Elias Papaconstantinou holds a Diploma in Chemistry from the University of Athens, Greece, 1960. After a year as Research Fellow at the, then, NRC Demokritos, he moved to the USA and obtained a PhD degree in inorganic chemistry with M. T. Pope from Georgetown University, Washington DC, 1968. He was Postdoctoral Research Fellow (1968–1970) at Boston University on the photochemistry of inorganic complexes and Chief Research Chemist at the Electronic Chemicals Division, Philip A. Hunt Chemical Corporation, NJ, USA, 1980–1972. He



Elias Papaconstantinou

joined the Institute of Physical Chemistry NCSR Demokritos in 1972 and was appointed Visiting Associate Professor at Boston University 1979–1980. He is currently Director of the Catalytic–Photocatalytic Processes Lab. His current research interests include redox catalytic processes, polyoxometallate, photocatalysis and environmental chemistry (Advanced Oxidation Processes).

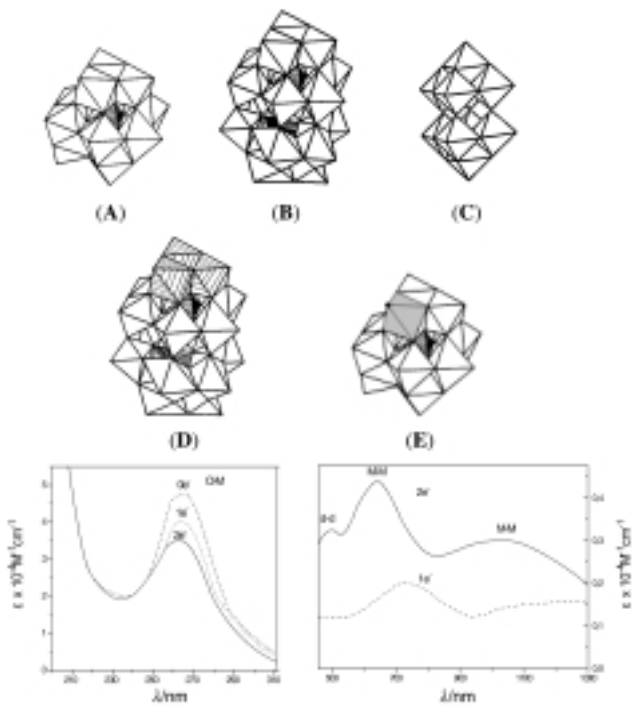


Fig. 1 Characteristic structures of POM. (A) $\text{PW}_{12}\text{O}_{40}^{3-}$, Keggin structure; (B) $\text{P}_2\text{W}_{18}\text{O}_{62}^{6-}$, Wells–Dawson structure; (C) The structure of the isopoly anion $\text{W}_{10}\text{O}_{32}^{4-}$. They are composed of WO_6 octahedra sharing corners and edges. In $\text{PW}_{12}\text{O}_{40}^{3-}$ the heteroatom P is within the central tetrahedron PO_4 . $\text{P}_2\text{W}_{18}\text{O}_{62}^{6-}$ arises from the Keggin anion, by removing three WO_6 octahedra and joining the two 9-tungsto half units. Also shown in this figure examples of: (D) Mixed POM with Wells–Dawson structure, for instance, $\text{P}_2\text{W}_{15}\text{Mo}_3\text{O}_{62}^{6-}$ in which three W atoms have been replaced by Mo atoms whose octahedra are shown hatched. (E) TMSP with Keggin structure, for instance $[\text{PW}_{11}\text{O}_{39}\text{Mn}(\text{H}_2\text{O})]^{6-}$. In the shaded octahedron, $-\text{W}-\text{O}$ moiety has been replaced by $-\text{Mn}-$ (H_2O). Several ligands, besides H_2O , can coordinate in the position shown as solid circle. Oxidized and reduced (by one and two electrons) spectra of $\text{PW}_{12}\text{O}_{40}^{3-}$. The $\text{O} \rightarrow \text{M}$ CT band, the intervalence electron transfer (M–M CT) and d–d transitions, are indicated on spectra.²

metal substituted POM (TMSP), for instance $[\text{PW}_{11}\text{O}_{39}\text{Mn}(\text{H}_2\text{O})]^{6-}$,^{1,2} [Fig. 1(E)].

POM have well defined structures and properties and their size is typically a few nm. They have diverse chemistry with applications in the field of analytical chemistry, biochemistry and solid state devices and have been used as antiviral and antitumor reagents. However, their most important property is in the field of catalysis.⁴ POM, like metal oxides, participate in catalytic processes as oxygen and multielectron relays. Several books and review articles have already described the development of POM and the field is expanding rapidly. New, larger compounds have been formed that, besides their structural interest, have other promising prospects.⁵

Although condensation produces a few metal oxide anions, as mentioned above, aggregates of various sizes can be formed by stirring or sonication of a variety of metal oxides, such as TiO_2 or WO_3 , in aqueous solution.⁶ Other methods such as chemical precipitation or controlled hydrolysis and subsequent polymerization can give materials of uniform size. Particulate systems are commonly distinguished by their size and fall into the two major categories of colloids and macroparticles. Macroparticles have a size that exceeds *ca.* 100 nm and form turbid suspensions, whereas colloids contain smaller particles that form clear solutions.⁷ In an excellent article Alivisatos described how the fundamental properties of these aggregates or clusters, vary, enormously, with size.⁸ Particles with a diameter over roughly 15 nm behave, generally, as bulk semiconductors (SC), whereas, smaller particles, of less than 5 nm have more or less molecular characteristics and are classified as quantum size clusters or quantum dots. Thus, POM, in SC terminology, may be considered ideal quantum size clusters, or quantum dots.⁸

Therefore, it is not surprising that these two systems exhibit overall similar behaviour.

It should be noted that despite determination of the Keggin and Wells–Dawson structures, mentioned below, many chemists, up until the Sixties, considered POM as inorganic polymers. A similarly unclear picture exists for the exact structure of metal oxide particulates. It is expected that these particles will resolve to definite structures, following the historical development of POM, but from the opposite direction, *i.e.*, from larger to smaller sizes.

2 Properties

In the last twenty years or so, we have seen important developments in the photochemistry and photocatalysis of semiconductors and, to a lesser extent, POM. Each of the various observations and explanations given for one group appears to have a counterpart in the other group. Yet, there are generally, (and unintentionally), no cross references between the two groups. This matter has improved recently as discussed below.

Some general points are worth mentioning. For instance:

(a) If one looks at the electronic absorption spectra of the oxidized and reduced WO_3 colloids and at their electrochemical behaviour, it can be seen that they have a pattern characteristic of polyoxotungstates,⁹ as others have also noticed,¹⁰ (Fig. 2). The case of TiO_2 is also similar.¹¹ The overall resemblance to the spectra of POM (shown in Fig. 1) is apparent. The blue color of reduced POM is thus attributed to intra electron transfer between adjacent metal ions, M–M charge transfer (CT) bands² and a somewhat similar explanation holds for the blue coloration of reduced WO_3 and TiO_2 .

(b) The band gap in SC, E_g (see below), is a function of the size of the metal oxide particulates. The smaller the size, the higher the E_g .⁸ A similar trend is noticed with POM as exemplified by the threshold and peak absorptions of the spectra of Keggin (ionic size *ca.* 7.2 nm³) and Wells–Dawson (ionic size *ca.* 10.3 nm³) structures of phosphomolybdates and phosphotungstates, that have overall similar characteristics [Fig. 3(A and B)].²

(c) It has been stated that accumulation of electrons on POM lowers the efficiency of photoreaction. For instance, in the photooxidation of propan-2-ol to propanone by $\text{PW}_{12}\text{O}_{40}^{3-}$, the efficiency drops by an order of magnitude in going from the oxidized 12-tungstophosphate, $\text{PW}_{12}\text{O}_{40}^{3-}$, to the form $\text{PW}_{12}\text{O}_{40}^{4-}$ that is reduced by one electron.¹² An analogous statement has been made for SC (TiO_2), namely, that accumulation of electrons on SC lowers the quantum yield¹³ by increasing the electron hole ($\text{h}^+ + \text{e}^-$) recombination rate (see below).

(d) Appreciable negative charge can be built up on metal oxide particulates in the absence of an acceptor. This is also true for POM, whose characteristic property is that they undergo multiple, stepwise, ‘reversible’ (from a chemical point of view) reductions without decomposition.²

(e) Accumulation of charge on SC drives the redox potential to more negative values, *i.e.*, the redox potential is a function of the charge density.¹⁴ This result was demonstrated, a long time ago for POM with the Keggin structure by Pope and Varga, (Fig. 4).¹⁵

(f) The rate-determining step in photocatalytic processes with metal oxide particulates was reported to be the removal of the electrons from the SC.¹³ Again, a similar statement has been made for POM, namely, that the rate-determining step in the photocatalytic cycle is the regeneration (reoxidation) of the catalyst.¹²

(g) Both systems, *i.e.*, polyoxotungstates and TiO_2 particulates, are effective photocatalysts for the mineralization to

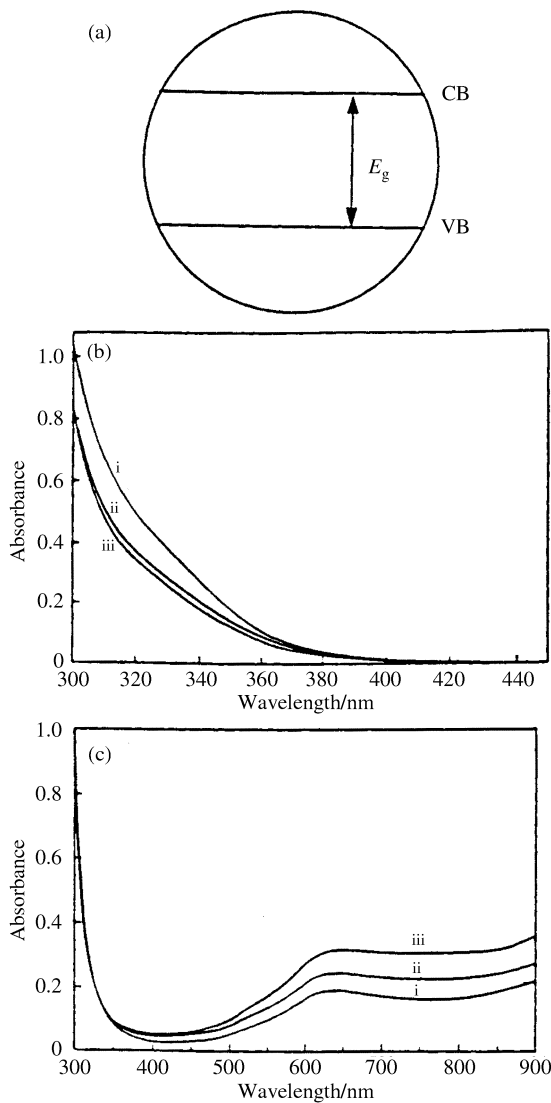


Fig. 2 (a) A metal oxide particle, *i.e.*, a SC, is usually represented as a circle with two bands: VB (valence band) and CB (conduction band), separated by the energy gap E_g ; see text. (b) Absorption spectra of WO_3 colloids (0.4 M) in water, with diameters 2–5 nm. The oxalic acid concentration that controls the size of the particles was i, 0.16, ii, 0.23 and iii, 0.31 M;⁹ (c) Absorption spectra of deaerated aqueous suspension of WO_3 colloids (0.4 M) following UV photolysis ($\lambda > 300$ nm) for 6 min., in presence of various concentrations of oxalic acid i, 0.16, ii, 0.23 and iii, 0.31 M. (Reprinted from reference 9, with permission.)

CO_2 , H_2O and inorganic anions of a great variety of organic pollutants (see below).

Thus, as mentioned earlier, the two systems have advanced independently, yet they exhibit great similarities, as is now quite obvious.

As always, the generalities break down when we get down to specifics. For POM the well defined properties, such as solubility, stability,¹ excited state life times,¹⁶ can be associated with the structure. Thus, for example, $\text{W}_{10}\text{O}_{32}^{4-}$ with a structure other than the Keggin and Wells–Dawson structure (Fig. 1), does not follow the rule of size, having *ca.* 450 and 320 nm for the threshold and peak absorptions, respectively [Fig. 3(C)].

No such specific properties can be noted for SC clusters for lack of structural data until now. In POM electrons are trapped in reasonably well understood molecular orbitals, so that reduced POM can be isolated, studied and prevented from undergoing further reactions. No such treatment is possible, so far, with band gap illuminated SC. For instance, most commercial SC samples have catalytic activity that varies from

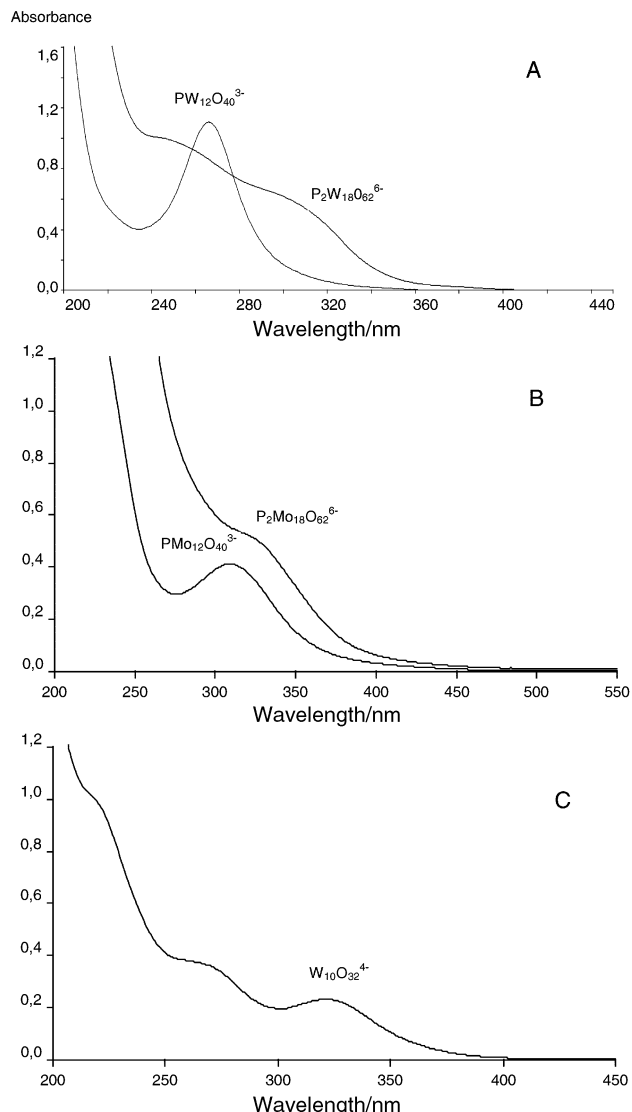


Fig. 3 Comparison of the spectra of the oxidized forms of: (A) $\text{PW}_{12}\text{O}_{40}^{3-}$ and $\text{P}_2\text{W}_{18}\text{O}_{62}^{6-}$; (B) $\text{PMo}_{12}\text{O}_{40}^{3-}$ and $\text{P}_2\text{Mo}_{18}\text{O}_{62}^{6-}$; (C) $\text{W}_{10}\text{O}_{32}^{4-}$. POM, *ca.* 2×10^{-5} M, in 50:50 $\text{CH}_3\text{CN}-\text{H}_2\text{O}$; 0.1 M HClO_4 .

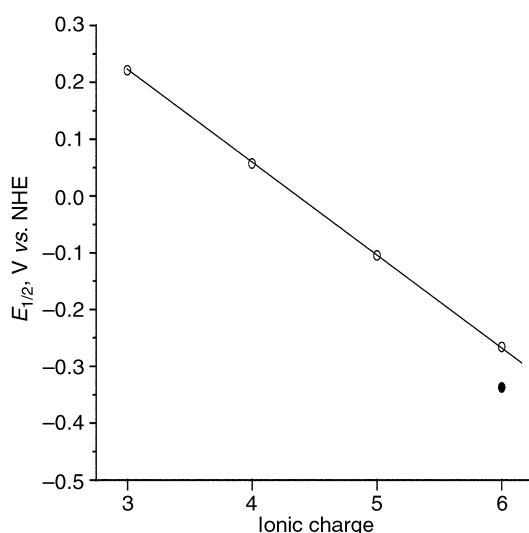


Fig. 4 Half-wave potentials for one-electron reduction *vs.* charge of the anions with Keggin structure: $\text{PW}_{12}\text{O}_{40}^{3-}$, $\text{SiW}_{12}\text{O}_{40}^{4-}$, $\text{FeW}_{12}\text{O}_{40}^{5-}$, $\text{CoW}_{12}\text{O}_{40}^{6-}$, $\text{H}_2\text{W}_{12}\text{O}_{40}^{6-}$ ●. (Reprinted from reference 15, with permission.)

batch to batch. In SC oxidations and reductions are not easily separated and cannot be stoichiometrically controlled.

3 Photochemical behaviour

The points listed above are some general thoughts and observations scattered in the literature, referring to either of the systems under discussion. It is the similarities in behaviour that we will focus upon, providing an overall picture of the parallel photochemical behaviour of these two categories of compounds in their reactions with organic substrates in aqueous solutions, as presented in the literature.

We will mainly consider the behaviour of TiO_2 and WO_3 as SC and that of polyoxotungstates as POM. A somewhat similar approach to the overall characteristics of POM and SC, but not to their specific photochemical behaviour, has been reported by Gomez-Romero;¹⁰ a comparison of several POM and semiconducting materials in CH_3CN has also been presented by Hill and Chambers.¹⁷ Maldotti *et al.* have mentioned the similarity between the behaviour of photoexcited WO_3 and TiO_2 with that of POM.¹⁸ We will present a few key points of the several that substantiate each case.

The following steps are encountered in the photochemistry and photocatalytic processes undergone by polyoxotungstates and metal oxide particulates.

3.1 Preassociation of catalysts with substrate

Several observations suggest the formation of a preassociated complex or a preassociated equilibrium of the catalyst with the organic substrate in aqueous solution,



where M is a polyoxotungstate or metal oxide particulate, and S an organic substrate. For POM the association is suggested by: (a) NMR data,¹⁹ (b) the rate constants ($10^{12} \text{ M}^{-1}\text{s}^{-1}$) for reaction of excited POM with substrate (*i.e.*, faster than diffusion-controlled),¹⁹ (c) X-ray data,²⁰ (d) electronic spectra^{10,17} and (e) the Langmuirian behaviour of the system.^{12,21} Incidentally, in all studies so far, high affinity of the organic compounds for POM has been observed (*i.e.*, high association constants). Evidence for this arises from the fact that even trace amounts of organic pollutants (*i.e.* of concentrations in the ppb range) undergo effective photodecomposition in homogeneous aqueous solutions containing POM (see below). For metal oxide particulates, the corresponding association is demanded by the fact that: (a) diffusion is too slow to compete with ($\text{e}^- + \text{h}^+$) recombination whose life time is in the order of nanoseconds. Thus the organic species must be preassociated with the catalyst before the arrival of the activating photon,²² see below and (b) the Langmuirian behaviour.²³ As far as the latter case is concerned, plots of initial rates of photoredox reactions as a function of increased concentration of organic substrate, for a certain concentration of catalyst, yield similar type of diagrams (Fig. 5). This means, as already mentioned, that both systems follow Langmuir–Hinshelwood behaviour or Michaelis–Menten kinetics. Thus, at low concentrations of organic substrate, the initial photoreaction is first order with respect to substrate, moving progressively (flat area) to zero order. This behaviour has been observed in every substrate tried so far with metal oxide particulates or POM and does not differ between semiheterogeneous systems, as encountered with metal oxide particulates, or homogeneous systems that use POM.

3.2 Excitation of the catalysts

In metal oxide particulates atomic and molecular orbitals coalesce to form energy bands. Impinging light $\lambda > E_g$ (E_g , the

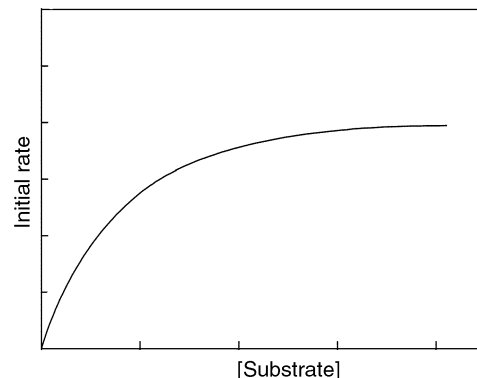
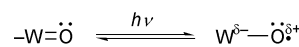


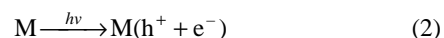
Fig. 5 Typical plot showing the variation in the initial rate of the photoredox reaction as a function of increased concentration of organic substrate, for a certain concentration of catalyst (metal oxide particulate or POM).

band gap energy of semiconductor) leads to electron hole separation (Fig. 2a).

By analogy, excitation into the $\text{O} \rightarrow \text{M}$ CT band of POM (near-visible and UV region), results in electron hole separation, which can be represented as



(where $-\text{W}=\text{O}$ represents a tungsten–oxygen bond in polyoxotungstates). Thus, for both systems the excited state can be described as



In eqn. (2), we have avoided the preassociated complex for reasons of clarity.

3.3 Photolysis in deaerated solutions

Excitation renders these systems powerful oxidizing reagents, able to oxidize a great variety of organic compounds. In the absence of electron trapping reagents (mainly dioxygen), electrons accumulate on metal oxide particulates, and POM, leading to the gradual development of a blue color, especially in the case of POM (Fig. 6). Noteworthy are the similarities in the photolysis spectra of deaerated aqueous solutions of $\text{PW}_{12}\text{O}_{40}^{3-}$ (Fig. 6)¹² and aqueous suspensions of WO_3 colloids in the presence of organic substrates,⁹ (Fig. 2c).

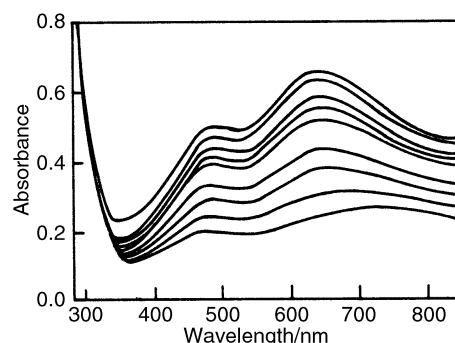
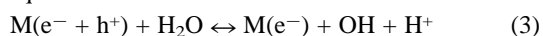


Fig. 6 Gradual development of a blue color, indicating the successive formation of one-electron (750 nm) and two-electron (650 nm) reduction products of $\text{PW}_{12}\text{O}_{40}^{3-}$, 0.1 mM; propan-2-ol, 2 mM in 0.1 M HClO_4 ; deaeration with Ar. Photolysis at 254 nm.

3.4 Formation of OH radicals upon photolysis of catalysts in aqueous solution

Reaction of the excited catalyst with H_2O (*i.e.* oxidative hole trapping) creates “surface” bound OH radicals, according to the following equation.



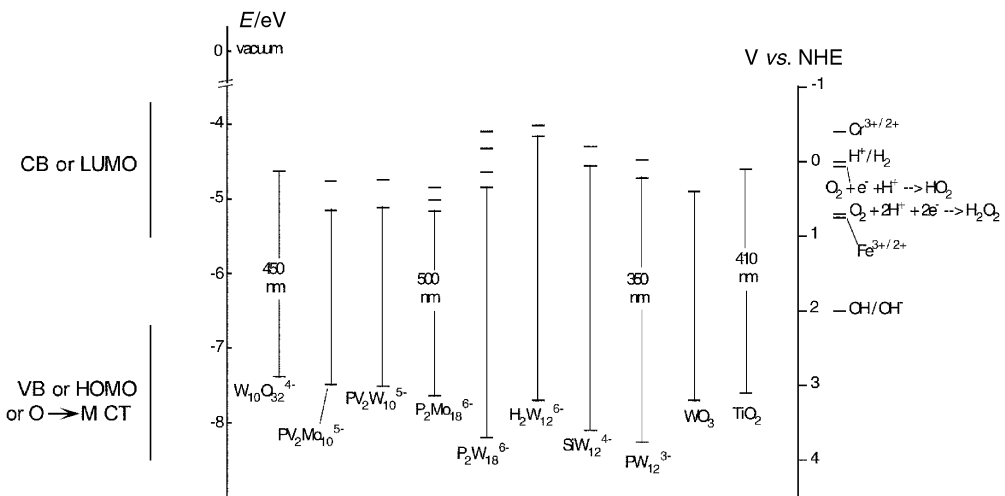
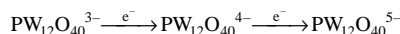


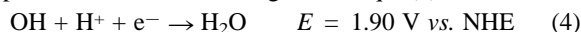
Fig. 7 Ground state and excited state redox potentials and corresponding energy levels, relative to vacuum and to NHE (normal hydrogen electrode), of some POM together with those of characteristic SC, WO_3 and TiO_2 , for comparison. Only the first few energy levels of POM are indicated on the diagram. For instance, for $\text{PW}_{12}\text{O}_{40}^{3-}$ (PW_{12}^{3-}) the first two energy levels are shown, corresponding to the following reactions:



Thus, the oxidizing ability of the ground state of $\text{PW}_{12}\text{O}_{40}^{3-}$ is 0.221 V vs. NHE (first reduction step), whereas the excited state potential is more positive by 350 nm (or $1240/350 \approx 3.5$ eV) more positive, *i.e.*, ≈ 3.7 V vs. NHE, as shown in the diagram and explained in the text.

The OH radicals react subsequently with substrates S in various ways, such that $\text{OH} + \text{S} \rightarrow$ hydroxylation, hydrogen abstraction, dehalogenation and oxidation products.

The following observations substantiate the formation of OH radicals: (a) OH adducts (hydroxylation products) have been detected in photolysis experiments with aromatic hydrocarbons in the presence of the POM^{21,24} and TiO_2 .^{25,26} Thus, for example, photolysis of phenol, whether in the presence of TiO_2 or $\text{PW}_{12}\text{O}_{40}^{3-}$ yields hydroquinone, catechol and 1,2,4-trihydroxybenzene (pyrogallol).²³ In principle, the hydroxylated product may originate from the hydrolysis of cation radicals produced from direct hole trapping by the organic adsorbate;²³ this subject is considered below. (b) ESR trapping experiments had detected OH radicals upon photolysis of POM^{18,27} and SC.²⁸ (c) The generation of OH radicals is also suggested by the fact that the excited state potentials of most POM and SC are more positive than the reaction given in eqn. (4).



To elaborate on this matter, we notice that excitation in SC promotes an electron from the valence band (VB) to the conduction band (CB), whereas in molecules (*i.e.* POM) the corresponding process is described as occurring from the highest occupied molecular orbitals (HOMO) to lowest unoccupied molecular orbitals (LUMO) or O→M CT band. If the threshold absorption is, say, 350 nm, for either SC or POM, the excited states will be better oxidants than the ground states by 350 nm or $1240/350 \approx 3.5$ eV.

Fig. 7 shows the ground state and excited state potentials of some POM together with those of characteristic SC for comparison. The excited state potential of POM was calculated from the equation: [excited state potential of POM (V vs. NHE)] = [ground state reduction potential of POM (V vs. NHE) + $1240/(\text{O}-\text{O})$ transition energy], where (O–O) transition energy is, roughly, the threshold absorption (nm) of the O→M CT band in the near-visible area.

To complete the argument in favour of OH radical formation, it has also been observed that the photodecomposition of trichloroacetic acid, which lacks α -hydrogen atoms, is much slower than that of chloroacetic acid (Fig. 8).²⁹ As is already known from radiation chemistry studies in aqueous solutions OH radicals attack preferentially α -hydrogen atoms.

Most of the metal oxides are large band gap semiconductors, as so are the polyoxotungstates. Thus, only light below 400 nm

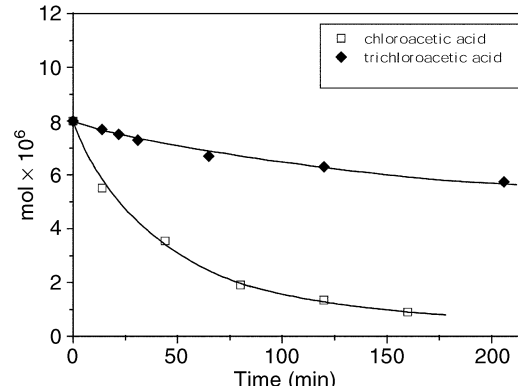


Fig. 8 Comparison of the photodegradation of ClCH_2COOH and CCl_3COOH upon photolysis of an oxygenated aqueous solutions of $\text{PW}_{12}\text{O}_{40}^{3-}$. Solution volume 4 mL; catalyst, 0.7 mM; substrate, 2 mM; pH 1.0 (HClO_4); $\lambda > 320$ nm. (Adapted from ref. 26, with permission).

is capable of producing electron hole pairs and so less than 5% of solar light can be utilized. One exception is iron(III) oxide with a band gap of 2.2 eV (for hematite $\alpha\text{-Fe}_2\text{O}_3$).²³ Hence, $\alpha\text{-Fe}_2\text{O}_3$ absorbs in the visible below 560 nm. However, its photocatalytic action is limited to a few cases. Other SC particles, namely, CdS and GaP , also absorb larger fractions of the solar spectrum, but these catalysts are degraded during repeated photocatalytic cycles.²³ Curiously enough, POM that absorb in the visible region, up to *ca.* 600 nm, such as molybdates, mixed tungstomolybdates and molybdoanvanades, have limited photocatalytic activity and are unstable.¹²

From a philosophical point of view it seems that Nature preserved this world by not activating various metal oxides with visible light that would have destroyed organic matter. It is this goal, *i.e.*, destruction of organic pollutants using solar light, that the scientific world is trying to achieve in a controlled manner.

3.5 Direct reaction of the excited state of the catalyst with substrate

The organic substrates, for both systems, act as adsorbed traps for the photogenerated holes either directly or through the

intermediacy of 'surface' hydroxyl radicals as mentioned earlier.

Diffuse reflectance flash photolysis has been employed to distinguish the products of direct electron transfer to TiO_2 in aqueous suspensions from those resulting from reaction with OH radicals. This, however, has not produced indisputable results.^{22,30}

3.6 Mineralization of organic pollutants.

Photodecomposition kinetics

The high oxidizing ability of the excited states and the formation of OH radicals by both polyoxotungstates and SC (TiO_2), as mentioned above, are the causes of photodegradation (to CO_2 , H_2O and inorganic anions) of a great variety of organic compounds.^{23,24} Thus mineralization has been reported in both systems for alcohols, aldehydes, ketones, acids, aromatic compounds substituted with Cl, Br, OH and for pesticides. Mineralization of carbon can be monitored through either the evolution of CO_2 or the disappearance of all the organic carbon. Over 1500 papers have been published on the ability of TiO_2 to cause mineralization, whereas the contribution of POM to the subject has been recognized only recently.^{21,24} Fig. 9 shows a

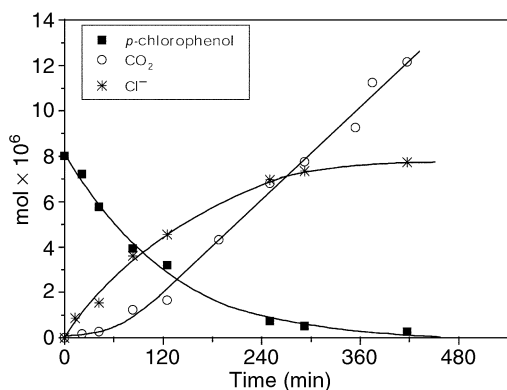


Fig. 9 Photocatalytic degradation and formation of Cl^- and CO_2 of an oxygenated aqueous solution of 4-chlorophenol in presence of $\text{W}_{10}\text{O}_{32}^{4-}$, 0.7 mM; pH, 2.5; $\lambda > 320$ nm. Photolyzed solution 4 mL.

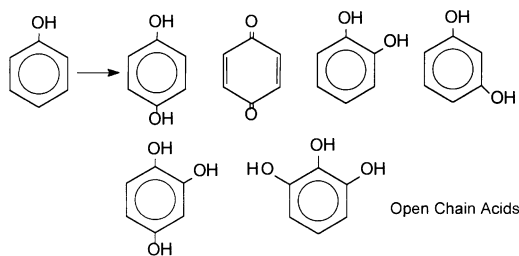
typical photodegradation process of chlorophenol, in which the disappearance of substrate and the formation of CO_2 and Cl^- are illustrated. It can be seen that CO_2 is detected after an induction period, as is observed for all aromatic substrates used so far, indicating that the process of mineralization goes through several intermediates before the opening of the aromatic ring. For both systems, the disappearance of organic compounds as a function of irradiation time obeys first-order kinetics.^{22,24}

3.7 Formation and decay of similar intermediates

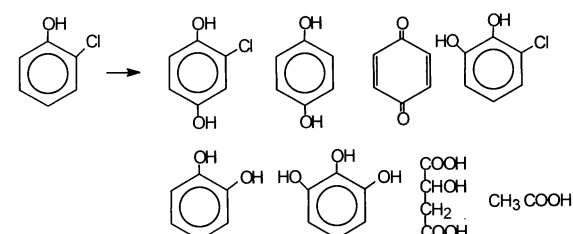
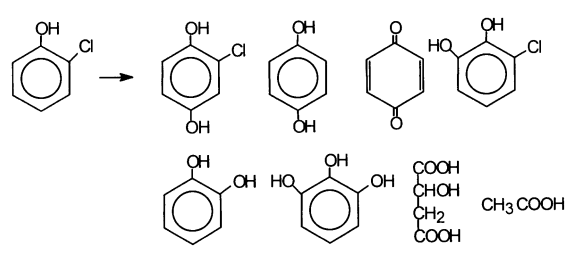
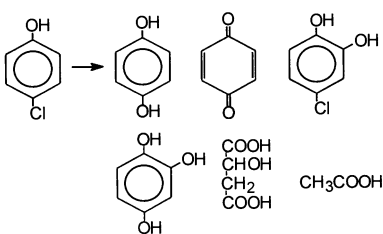
The process of mineralization, for both categories of catalysts, passes through the formation and decay of several similar intermediates. This is to be expected, since their oxidizing ability is exercised mainly through OH radicals, as mentioned earlier. Thus, the characteristic reactions of OH radicals have been encountered: (a) hydroxylation of aromatic compounds (*i.e.* OH adducts) as mentioned earlier; (b) H-abstraction; (c) dehalogenations; (d) decarboxylations; (e) breaking of the aromatic ring and formation of short-chain aliphatic acids. Also addition or transfer of hydrogen atoms is observed.

We present below examples of common intermediates encountered in the photodecomposition of, for example, phenol,^{23,31} (Scheme 1) and chlorophenols.^{24,32} (Scheme 2).

The formation of CH_2 and CH_3 groups from aromatic carbon (*i.e.* CH groups) implies that in the photocatalytic processes



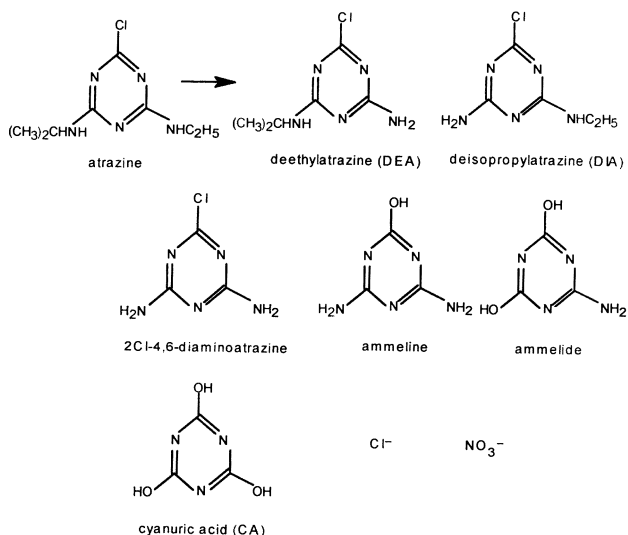
Scheme 1 Common intermediates detected during photodegradation of phenol by polyoxotungstates and TiO_2 . (Reprinted from ref. 31, with permission from Elsevier Science).



Scheme 2 Intermediates detected during the course of mineralization of chlorophenols by both systems. (Reprinted from ref. 24, with permission from Elsevier Science).

promoted by POM and TiO_2 there is a reductive (hydrogenation) pathway, in addition to the oxidative process. On the other hand, the formation of aliphatic acids and the ultimate formation of CO_2 by both systems implies addition of OH radicals to the organic ring, leading to the formation of CO bonds or hydration of the oxidized organic radical cation.^{23,24}

An interesting case that also demonstrates the similarity of these processes is the photocomposition of nitrogen containing aromatic rings. In particular, the initial photodecomposition of atrazine, by both methods, takes place within a few minutes, leading, within a few hours, to cyanuric acid (CA). However, the latter resists photodegradation for tens of hours in the presence of either TiO_2 or polyoxotungstates.^{33,34} Scheme 3 shows the main common intermediates identified in the photodegradation processes of atrazine by the two systems and the final products. Notice that in both cases, the chlorine groups end up as chloride ions and amine nitrogen atoms as nitrate ions.



Scheme 3 The main common intermediates and final products detected in the photodecomposition of atrazine by TiO_2 and polyoxotungstates.

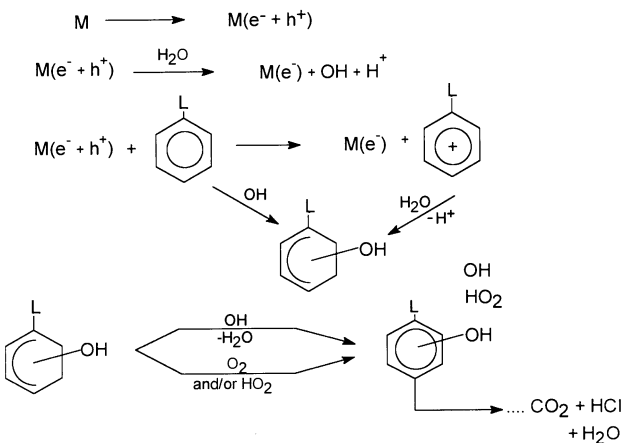
We mentioned earlier that, getting down to specifics, the two processes might present differences. In this respect, we note that Texier *et al.*³⁴ working with TiO_2 and $\text{W}_{10}\text{O}_{32}^{4-}$, in the photodecomposition of atrazine, have identified with TiO_2 two transient amides, which they did not observe with $\text{W}_{10}\text{O}_{32}^{4-}$. Even in this case, the authors point out that these amides might be too reactive toward $\text{W}_{10}\text{O}_{32}^{4-}$ and so their steady-state concentration could be too low to be detected. A more serious argument on their part is that they doubt the formation of OH radicals with $\text{W}_{10}\text{O}_{32}^{4-}$. They argue that in absence of organic substrate, H_2O_2 should have been detected. We think that even in the case of $\text{W}_{10}\text{O}_{32}^{4-}$ whose excited state life time is longer than those of most POM¹⁶ the indirect rate of electron hole recombination,



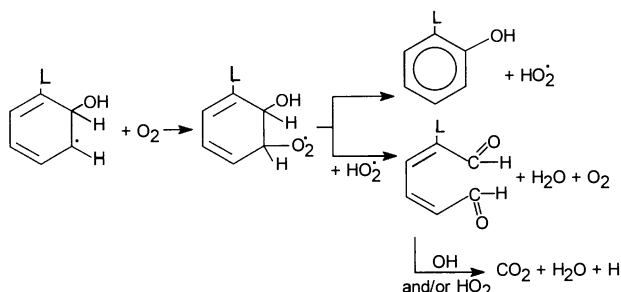
does not allow the 'surface' bound OH radical to escape to the bulk of the solution to encounter another OH radical for the formation of H_2O_2 .

3.8 Degradation pathways

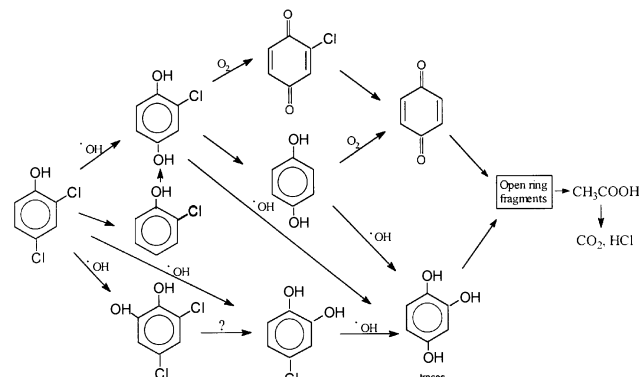
As has been mentioned earlier, hydroxylated products may, in principle, arise from direct reaction of the aromatic ring with OH radicals and/or from the hydrolysis of the oxidized cation radical generated by direct hole transfer to the associated organic substrate, or to put it in more familiar chemical terminology, by direct electron transfer from the associated organic substrate to the photoexcited catalyst. Scheme 4 shows the common pathway of photodecomposition of an L-substituted aromatic compound as used by several workers working with OH radicals produced in aqueous solutions from $^{60}\text{Co}-\gamma$ -radiolysis, TiO_2 photolysis or POM.²⁴ Scheme 4 provides details of the fate of the organic substrate, accounting for the formation of hydroxy aromatic derivatives and the overall mineralization process.²⁴ For an *ortho* OH addition in the L-substituted benzene ring above, the reactions depicted in Scheme 5 explains, according to Matthews,²⁶ the mineralization process. Dioxygen is also involved, the role of which is considered below. Finally, a more specific example is the photodecomposition of 2,4-dichlorophenol.³⁵ Several common intermediates, identified in the decomposition by both systems, necessitate the degradation pathway shown in Scheme 6.



Scheme 4 The common pathway of photodecomposition of an L-substituted aromatic compound, as used by several workers working with OH radicals. (Reprinted from ref. 24, with permission from Elsevier Science).



Scheme 5 The mechanism of mineralization after an *ortho* OH addition in the L-substituted benzene ring, showing, also, the participation of dioxygen, according to Matthews.²⁶ (Reprinted from ref. 24, with permission from Elsevier Science).



Scheme 6 Photodegradation pathway according to the common intermediates found in the photocatalytic decomposition of 2,4-dichlorophenol by both systems. (Reprinted from ref. 35, with permission from Elsevier Science).

3.9 Regeneration of catalysts

Both systems can serve as electron relays, *i.e.* they are able to transfer the accumulated electrons to a variety of compounds with a less negative reduction potential than the conduction band of SC or the highest occupied molecular orbital (HOMO) of POM and thus close the photocatalytic cycle, which is represented for both systems in Fig. 10. For both categories of catalysts, the rate-determining step in the photocatalytic cycle has been reported to be the reoxidation (regeneration) of catalyst.^{12,13}

Generally, photocatalytic reductions with SC (TiO_2) are less frequently encountered than are oxidations, probably because, as has been stated, the reducing ability of the conduction band

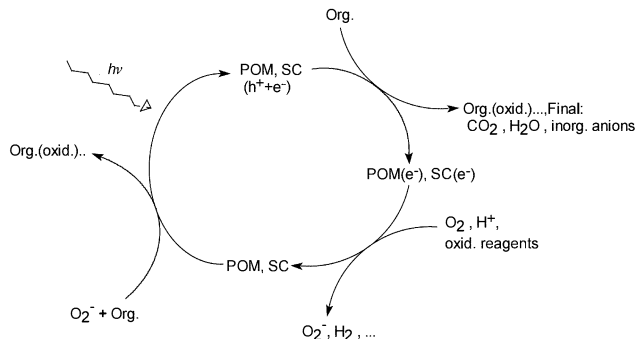
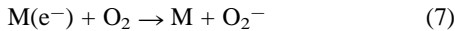


Fig. 10 The photocatalytic cycle representing the reactions involved for both POM and SC.

electrons is significantly lower than the oxidizing ability of a valence band hole.³⁰ This also holds true for POM as one can see from the redox potential of Fig. 7 and for one further reason: POM are in the d^0 electronic state (*i.e.* the highest, W^{6+} , oxidation state); therefore there are no electrons available for reduction.

Hole oxidation of organic compounds accumulates electrons on the catalyst, which can be delivered to various reducible species in the solution. Thus, for instance, H^+ has been reported to be reduced to H_2 ,^{12,30} haloaromatics undergo reducible dehalogenation^{23,24} and nitrobenzene has been reported to be reduced to aniline.

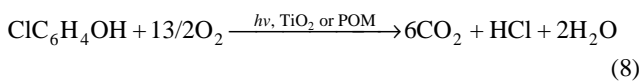
Various oxidants have been used as photoelectron traps (or oxidizing reagents for reduced catalysts) such as $S_2O_8^{2-}$, IO_4^- , BrO_3^- , ClO_3^- and H_2O_2 .²³ Dioxygen is the most effective and the cleanest electron trapping reagent for both types of catalysts. In the process, the superoxy radical is formed,



which may further participate in the oxidation processes^{24,29} (Fig. 10 and Scheme 5).

4 Conclusions

(a) Metal oxide particulates and POM upon excitation with near visible and UV light serve as photocatalysts in a variety of similar processes. (b) For photoreaction to occur, before deactivation of the excited catalyst takes place, both systems require the formation of a preassociated complex or preassociation equilibrium or, for that matter, a supramolecular species between the catalyst and substrate. (c) For both systems, the rates of photooxidation of substrate are the result of two competitive reactions: (i) direct reaction of the excited catalyst with substrate and (ii) reaction through OH radicals. (d) Both systems cause mineralization (*i.e.* formation of CO_2 , H_2O and inorganic anions) of a great variety of organic pollutants, *via* similar intermediates. (e) The photodecomposition rates obey first-order kinetics with respect to the organic species. (f) For both systems, the rate-determining step in the photocatalytic cycle has been reported to be the regeneration (reoxidation) of the catalyst with dioxygen being the most effective and the cleanest oxidizing reagent. (g) Using chlorophenol as an example, the overall photodecomposition reaction is



Acknowledgements

We thank The Ministry for Development, General Secretariat of Research and Technology for financing part of this work.

References

1. L. C. W. Baker and D. C. Glick, *Chem. Rev.*, 1998, **98**, 3.
2. M. T. Pope, *Heteropoly and Isopoly Oxometalates in Inorganic Chemistry Concepts* 8, ed. C. K. Jorgensen, M. F. Lappert, S. J. Lippard, J. L. Margrave, K. Niedenzu, H. Noth, R. W. Parry and H. Yamatera, Springer Verlag, West Berlin, 1983.
3. F. A. Cotton and G. Wilkinson, *Advanced Inorganic Chemistry*, J. Wiley and Sons, New York, 5th edn, 1988, 776–819.
4. M. T. Pope and A. Muller, *Angew. Chem., Int. Ed. Engl.*, 1991, **30**, 34.
5. A. Muller, F. Peters, M. T. Pope and D. Gatteschi, *Chem. Rev.*, 1998, **98**, 239.
6. M. R. Hoffmann, T. S. Martin, W. Choi and D. W. Bahnemann, *Chem. Rev.*, 1995, **95**, 69.
7. M. Gratzel, *Photocatalysis and Environment*, ed. M. Schiavello, NATO ASI Series, Kluwer, Dordrecht, 1987, pp. 367–398.
8. A. P. Alivisatos, *Science*, 1996, **271**, 933.
9. I. Bedja, S. Hotchandani and P. V. Kamat, *J. Phys. Chem.*, 1993, **97**, 11064.
10. P. Gomez-Romero, *Solid State Ionics*, 1997, **101**, 243.
11. G. Rothengruber, J. Moser, M. Gratzel, N. Serpone and D. K. Sharma, *J. Am. Chem. Soc.*, 1985, **107**, 8054.
12. E. Papaakonstantinou, *Chem. Soc. Rev.*, 1989, **16**, 1 and references therein.
13. H. Gerischer and A. Heller, *J. Phys. Chem.*, 1991, **95**, 5261.
14. M. T. Nenadovic, T. Rajh, O. I. Micic and A. J. Nozik, *J. Phys. Chem.*, 1984, **88**, 5827.
15. M. T. Pope and G. M. Varga, *Inorg. Chem.*, 1966, **5**, 1249.
16. C. Tanielian, *Coord. Chem. Rev.*, 1998, **178–180**, 1165 and references therein.
17. R. C. Chambers and C. L. Hill, *Inorg. Chem.*, 1991, **30**, 2766.
18. A. Maldotti, R. Amadelli, G. Varani, S. Tollar and F. Porta, *Inorg. Chem.*, 1994, **33**, 2968.
19. M. A. Fox, R. Cardona and E. Gailard, *J. Am. Chem. Soc.*, 1987, **109**, 6347.
20. E. Coronado, J. R. Galan-Mascaro and C. Gimenez-Saiz, *J. Am. Chem. Soc.*, 1998, **120**, 4671 and references therein.
21. H. Einaga and M. Misono, *Bull. Chem. Soc. Jpn.*, 1996, **69**, 3435.
22. P. Pichat, *Handbook of Heterogeneous Catalysis*, eds. G. Ertl, H. Knozinger and J. Weitkamp, Wiley-VCH, New York, 1997, vol. 4, pp. 2111–2122.
23. D. Bahnemann, J. Cunningham, M. A. Fox, E. Pelizzetti, P. Pichat and N. Serpone, *Aquatic and Surface Photochemistry*, eds. G. R. Helz, R. G. Zepplin and D. G. Grosby, Lewis Publ., Boca Raton, 1994, pp. 261–316.
24. A. Mylonas and E. Papaconstantinou, *J. Photochem. Photobiol. A*, 1996, **94**, 77 and references therein.
25. D. F. Ollis, C.-Y. Hsiao, L. Budiman and C.-L. Lee, *J. Catal.*, 1984, **88**, 89.
26. R. W. Matthews, *J. Catal.*, 1988, **111**, 264.
27. T. Yamase and T. Kurozumi, *J. Chem. Soc., Dalton Trans.*, 1983, 2205.
28. M. Anpo, T. Shima and Y. Kubakawa, *Chem. Lett.*, 1995, 1799.
29. A. Mylonas, A. Hiskia and E. Papaconstantinou, *J. Mol. Catal.*, 1996, **114**, 191.
30. M. A. Fox and M. T. Dulay, *Chem. Rev.*, 1993, **93**, 341.
31. A. Mylonas, V. Roussis and E. Papaconstantinou, *Polyhedron*, 1996, **15**, 3201.
32. G. Al-Sayed, J.-C. D’Oliveira and P. Pichat, *J. Photochem. Photobiol. A*, 1991, **58**, 99.
33. C. Minero, V. Maurino and E. Pelizzetti, *Res. Chem. Intermed.*, 1997, **23**, 291.
34. I. Texier, J. Ouazzani, J. Delaire and C. Giannotti, *Tetrahedron*, 1999, **55**, 3401.
35. A. Hiskia, E. Androulaki, A. Mylonas, S. Boyatzis, D. Dimotikali, C. Minero, E. Pelizzetti and E. Papaconstantinou, *Res. Chem. Intermed.*, 2000, **26**, 235.